

CONTACT PROBLEMS INCORPORATING ELASTIC LAYERS

D. NOWELL and D. A. HILLS

Department of Engineering Science, University of Oxford, Parks Road,
Oxford OX1 3PJ, U.K.

(Received 18 March 1987; in revised form 4 June 1987)

Abstract—In this paper, plane elastic contact between a thin strip and symmetric rollers is considered. Various loading regimes, including frictional sliding, frictionless and frictional indentation, and the effect of applying a tangential force less than that necessary to cause sliding are treated. For each case, the surface tractions are found, and, for the last two problems, a detailed analysis of the stick and slip zones is presented.

INTRODUCTION

The motivation for the present analysis was a desire to assess the degree of approximation implicit in representing the strip used in fretting fatigue tests as a half-plane. A schematic view of the geometry is shown in Fig. 1(a). Previous analyses had treated the contact as Hertzian, i.e. it had been assumed that the thickness of the strip was much greater than the contact semi-width, so that each body could be approximated by a half-plane [1, 2]. It transpires that for practical cases, where this ratio is typically 10, the idealization is entirely justified, but a wide variety of other cases with the same general layout, and where the assumption of Hertzian contact is certainly inappropriate, have also been examined.

Elastic contact problems involving strips can, in principle, be formulated using Sneddon's integral transform methods [3]. However, in practice two problems arise; first, the integrals developed are often difficult to evaluate accurately, since they are over a semi-infinite range and incorporate slowly decaying oscillatory kernels. Secondly, mixed boundary value problems cannot readily be formulated. Instead, a hybrid method due to Bental and Johnson [4] is adopted.

Whereas in half-plane problems an integral equation relating the surface displacements to a continuously varying traction distribution can easily be composed [5], for strip problems this is not feasible, owing to the complexity of the influence function. Instead, a piecewise linear idealization of the true traction is utilized, which consists of a series of overlapping triangles (Fig. 2). The first step in the solution is to determine the surface displacements at some point m due to a triangle of traction (direct or shear) centred on a point n . When this building block has been established, a wide variety of contact geometries may be analysed by formulating what is, essentially, a discretized form of the integral equation method. Details of the derivation of these influence functions are given by Bental and Johnson [4] and here, after summarizing the results needed, we concentrate on the solution of the boundary value problems.

INFLUENCE FUNCTIONS

The problem outlined above where two cylinders indent a strip as shown in Fig. 1(a) has the following surface boundary conditions outside the contact:

$$\sigma_{yy} = \tau_{xy} = 0 \quad |x| > a, \quad y = \pm b \quad (1)$$

where a is the contact semi-width and b the strip semi-thickness. We may use arguments of symmetry about $y = 0$ to augment eqn (1), giving the following:

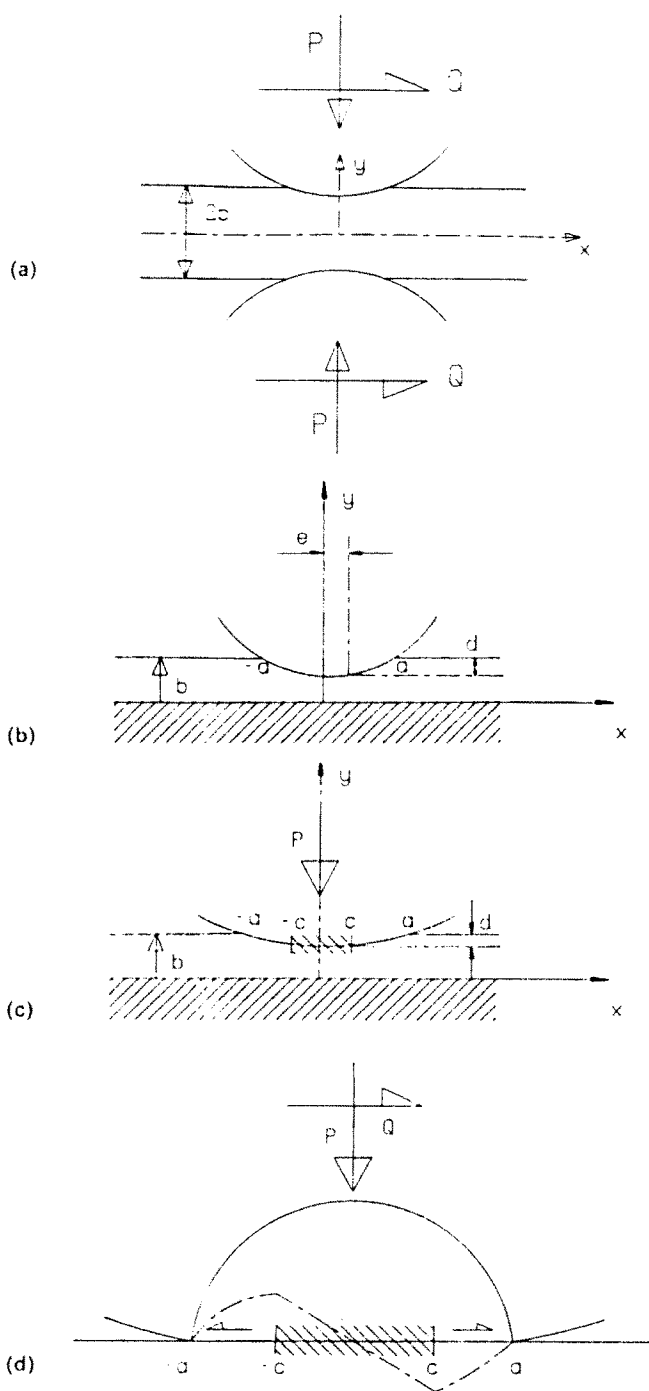


Fig. 1. Contact configurations.

$$\sigma_{yy} = \tau_{xy} = 0 \quad |x| > a, \quad y = b \tag{2}$$

$$\tau_{xy} = t = 0 \quad y = 0 \tag{3}$$

whereupon the problem is seen to be identical to that of an elastic strip of thickness b resting on a rigid frictionless substrate as shown in Fig. 1(b).

In general, coupling between shear and direct tractions may lead to an asymmetric distribution of direct traction. This would result in the centre of contact not being coincident with the centre of the indenter. Accordingly we take the origin as the centre of the contact and assume the centre of the indenter to be displaced by an amount e . To reduce

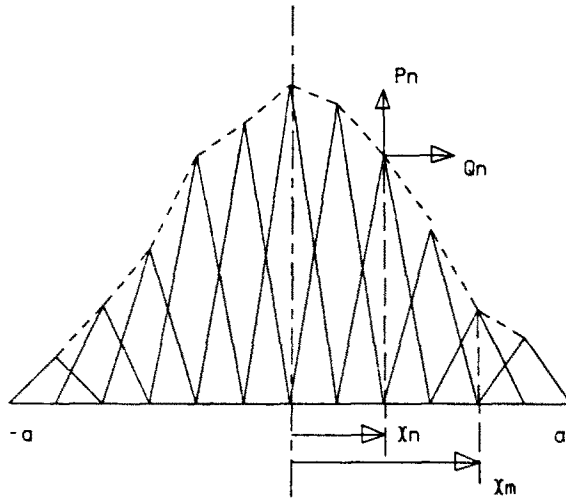


Fig. 2. Discretized model of surface tractions.

the number of independent variables we consider here contact between a cylinder and an elastic strip having the same elastic constants, namely Poisson's ratio ν and modulus of rigidity μ . The problem is formulated below for conditions of plane strain.

Direct and shear tractions over the contact are each represented by $2S$ overlapping triangles with equal bases (Fig. 2). The heights of the n th triangles are p_n and q_n , which represent the magnitudes of the direct and shear tractions, respectively, at $x = na/S$. We now write down the relative vertical and horizontal displacements $v(m)$, $u(m)$ due to the total direct and shear force exerted[4]

$$\begin{aligned} \frac{v(m)}{a} = & \sum_{n=(x-1)}^{x-1} P_n \left[\frac{B}{2} \{I_{AO} + I_A(m-n)\} + \frac{1}{2S} \{I_{AR}(m-n) - I_{AR}(n)\} + \frac{1}{2S} I_{AR}(m-n) \right] \\ & - \sum_{n=(x-1)}^{x-1} Q_n \left[\frac{B}{2} I_B(m-n) - \frac{1}{8S} \frac{1-2\nu}{1-\nu} I_{BR}(n) \right] \end{aligned} \quad (4)$$

$$\begin{aligned} \frac{u(m)}{a} = & \sum_{n=(x-1)}^{x-1} P_n \left[\frac{B}{2} \{I_B(m-n) + I_B(n)\} \right] \\ & - \sum_{n=(x-1)}^{x-1} Q_n \left[\frac{B}{2} \{I_D(m-n) - I_D(n)\} - \frac{1}{S} \{I_{AR}(m-n) - I_{AR}(n)\} \right] \end{aligned} \quad (5)$$

where $P_n = p_n/\bar{p}$, $Q_n = q_n/\bar{p}$, $\bar{p} = P/2S$, $B = b/a$ and functions I are precisely as defined by Bentall and Johnson, q.v., and tabulated for convenience in the Appendix.

Following Hertz, the relative vertical displacement within the contact zone is approximated by a parabola. An allowance is made for the eccentricity e , so that

$$\frac{v(m)}{a} = \frac{2DRA^2}{a} + \frac{2mEA^2}{S} - \frac{m^2 A^2}{S^2} \quad (6)$$

where $E = e/a$, $D = d/a$ (d being the rigid body normal approach), $A = a/a_x$ (a_x being the contact half-width predicted by the Hertzian solution), and R is the radius of the cylinder. Restrictions on the variation of the relative tangential displacement depend on the exact contact configuration. Note that within a stick zone the relative tangential strain ϵ_r (i.e. $\epsilon_{xx}^{\text{indenter}} - \epsilon_{xx}^{\text{strip}}$) between adhered points is equal to the value when they first entered the stick zone whilst in the slip zones the direct and shear tractions are related by the coefficient of friction, f , i.e.

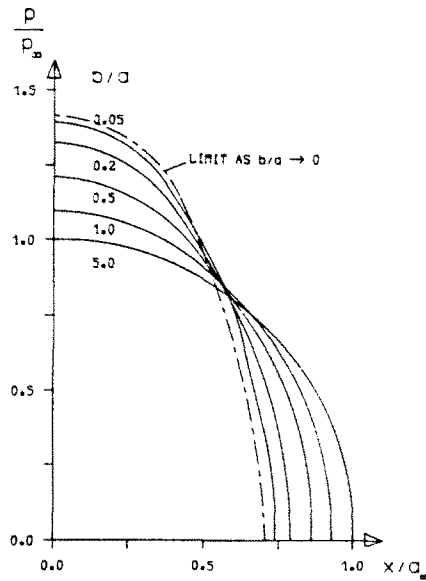


Fig. 3. Frictionless indentation: direct tractions (symmetric).

$$q = \pm |fp|. \quad (7)$$

FRICTIONLESS INDENTATION

The simplest problem which may be treated is normal indentation by a frictionless cylinder (Fig. 1(b)). At low loads, i.e. $a \ll b$, the contact is Hertzian, since the strip approximates a half-plane. At finite loads, the numerical solution must be used. Equations (4) and (6) are equated for all values of $-S \leq m \leq S$. Thus the vertical displacement is matched at $2S+1$ points, including the edges of contact. A further equation arises from the requirement of vertical equilibrium, i.e.

$$\sum_{n=-(S-1)}^{S-1} P_n = P/\bar{p} = 2S. \quad (8)$$

The unknowns are the $2S-1$ ordinates of the contact pressures P_n , together with the rigid body normal approach d , A (a measure of the contact patch size) and the eccentricity e . Thus the problem has been reduced to $2S+2$ simultaneous equations in $2S+2$ unknowns and may readily be solved using a computer library routine. As expected from symmetry e is found to be zero. The distribution of normal traction is shown in Fig. 3 for several values of b/a . P is normalized with respect to p_x , the maximum Hertzian contact pressure and the results were calculated with $S = 20$. The major effect of the finite thickness can be seen to be a reduction in contact area, compared to the Hertzian solution and a corresponding increase in peak pressure. The limiting case for large b/a is Hertzian contact of a cylinder on a half-plane. The opposite limit ($b/a \rightarrow 0$) corresponds to Hertzian contact of two cylinders of radius R ($a/a_x = 1/\sqrt{2}$, $p_{max}/p_x = \sqrt{2}$). This is as expected since for thin strips the displacements within the strip are small compared with those in the cylinders.

SLIDING CONTACT

Consider now quasi-static sliding contact between the impressed cylinder and the strip. Numerical solution is again achieved by combining eqns (4) and (5) and using eqn (7). In this case there is no longer symmetry, and e is non-zero. Again there are $2S+2$ knowns and unknowns (if only the $(2S-1)P_n$ are treated as unknown tractions) and the shear

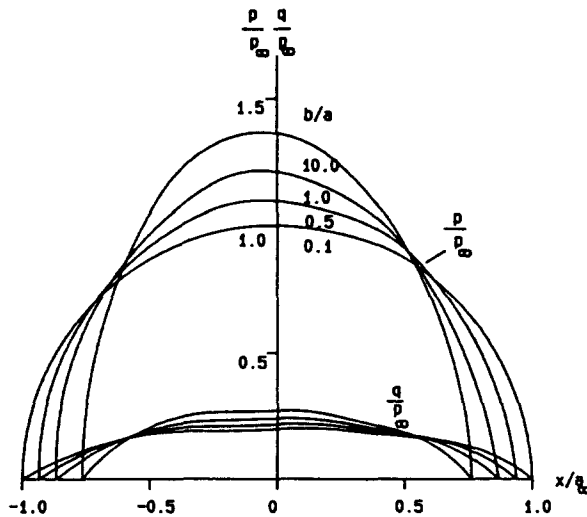


Fig. 4. Sliding contact, $f = 0.3$, $\nu = 0.3$: surface tractions.

components are related by eqn (7) (i.e. $q = fp$). Figure 4 shows distributions of normal and shear tractions at several different values of b/a for $f = 0.3$ and $\nu = 0.3$. These results were obtained with $S = 10$.

Again the major effect of the finite strip thickness can be seen to be a reduction in the contact area and an increase in the peak pressure. The coupling between shear and direct tractions produces some asymmetry in the results but the effect is not large at this value of f .

ADHESIVE INDENTATION

As a prelude to analysing the fretting problem, normal indentation where the interfacial friction is finite but $Q = 0$ will be treated. This configuration is considerably more complex than the previous ones, and a satisfactory initial simplification of the problem is to assume that the coefficient of friction is sufficiently high to prevent relative displacement between corresponding points on the two bodies once within the contact zone, i.e. that no slip takes place. As the applied load is increased, the contact patch grows and new surface particles come into contact. The relative strain between such points remains constant once they enter the contact and, since there is no rigid body tangential displacement, the relative displacement u_r also remains constant. We therefore need to ensure that, for all pairs of adhered points, u_r remains at the same value as when the two points entered the contact.

One difficulty is that the displacements of such points before they enter the contact zone are not known *a priori*. Further, since the displacement of points within the strip is an unknown function of the ratio b/a , the problem is not self-similar, unlike those treated by Spence[6, 7], and hence an incremental solution, as first used by Goodman in his analysis of contact between dissimilar spheres[8], is necessitated.

The solution proceeds as follows: at large values of b/a the geometry approximates to the Hertzian case of two half-planes and we thus expect the values of u_r to be small within the contact. It is therefore reasonable to assume an approximately linear variation of u_r with x for some large value of b/a ($= b/a_0$, say). We are then able to specify the relative tangential displacements at the matching points (u_m) in terms of the values at the edges of the contact $u(a_0)$, $u(-a_0)$, which are as yet unknown. We thus obtain the $2S+1$ tangential matching equations by substituting for u_m in eqn (5). There are now $4S+3$ equations, and the corresponding unknowns are: $2S-1$ values of P_n , $2S-1$ values of Q_n , E , A , D , $u(a_0)$, and $u(-a_0)$.

The solution reveals the values of u at $x/b = \pm a_0/b$. We now take a small load increment such that the contact grows to $x = \pm a_1$. Linear interpolation of the previous solution is used to determine u_m for all matching points within the range $|x| \leq a_0$ and the variation over the small intervals $a_0 \leq |x| < a_1$ is assumed linear. The solution of the second

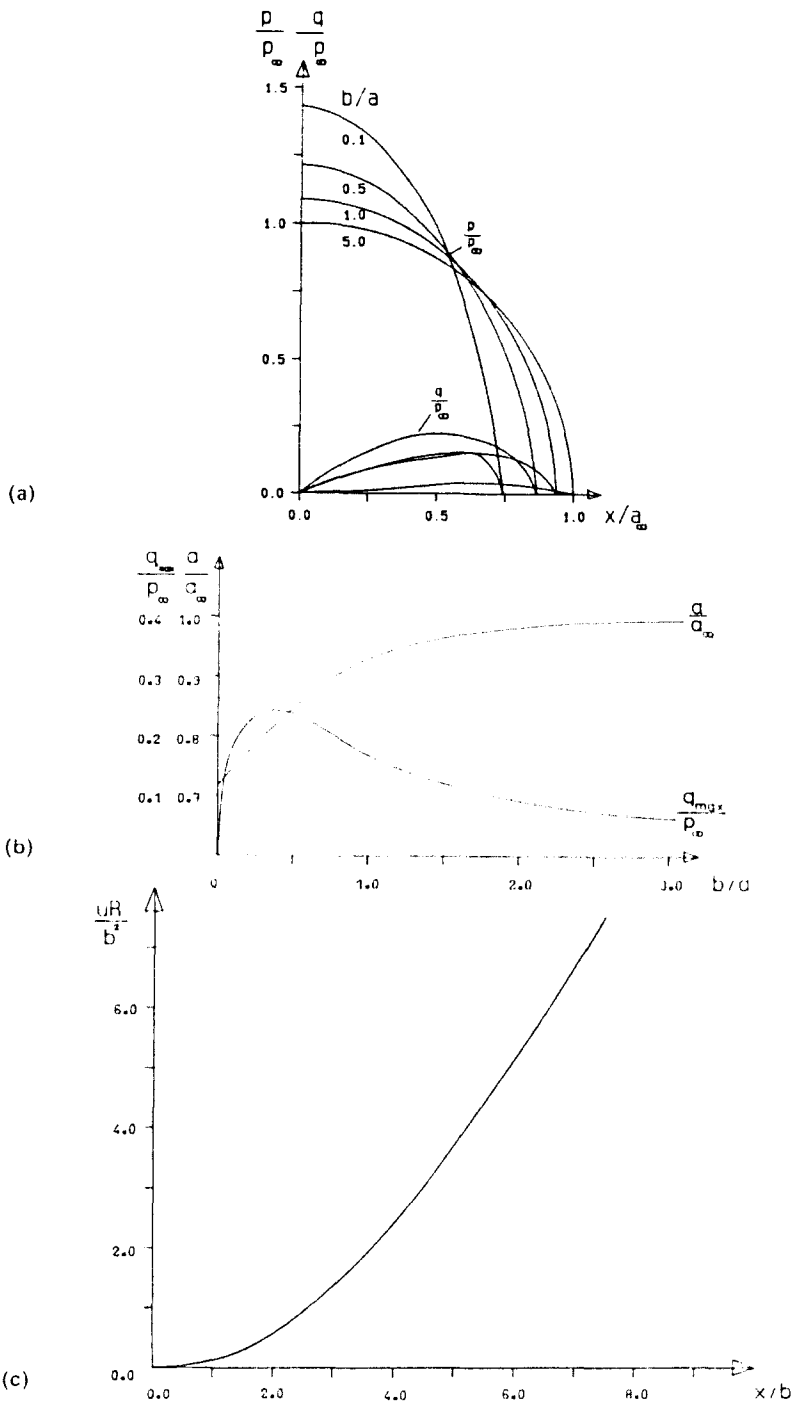


Fig. 5. Adhesive indentation, $\nu = 0.3$: (a) direct tractions (symmetric), and shear tractions (anti-symmetric); (b) variation of contact size and maximum shear traction with b/a ; (c) variation of relative tangential displacement with v within the contact.

step can now be found since the values of u_m at all matching points are either known from the previous solution or can be expressed in terms of $u(\pm a_1)$. Hence, the incremental solution proceeds by taking small steps in b/a from an initial value which is sufficiently large for the variation of u_r to be assumed linear. Once four values of $u(a_i)$ are known a fitted cubic spline is used in place of linear interpolation to determine u_m .

Results were calculated with $S = 10$ and for $\nu = 0.3$. Figure 5(a) shows the normal and shear stress distributions for various values of b/a . Figure 5(b) shows the variation of a/a_0 , and the maximum shear traction with b/a . It will again be noted that as $b/a \rightarrow 0$, and

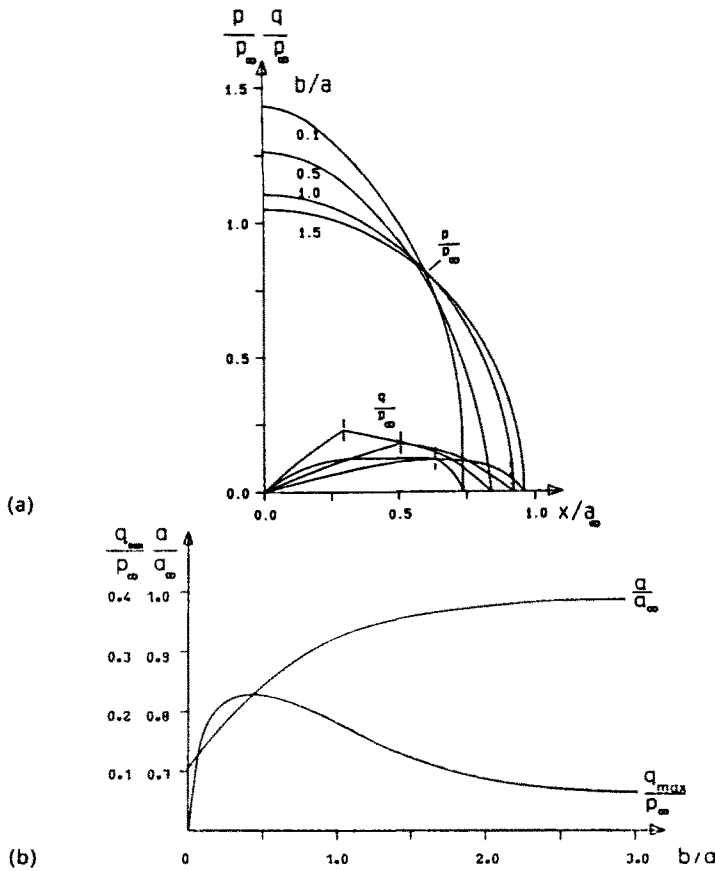


Fig. 6. Frictional indentation, $\nu = 0.3, f = 0.2$: (a) direct tractions (symmetric), and shear tractions (antisymmetric); (b) variation of contact size and maximum shear traction with b/a , which, for adhesive indentation, is the entire contact.

$b/a \rightarrow \infty$ the contact becomes Hertzian. Between these limits, the finite strip causes significant shear tractions at the interface which reach a maximum at $b/a \approx 0.35$. Figure 5(c) shows the variation of u with x within the stick zone.

FRICIONAL INDENTATION

The restriction that the coefficient of friction is sufficiently high to sustain stick throughout the contact is now relaxed. It has been shown by Goodman[8], for the case of point contact between dissimilar bodies, that although the shear traction falls continuously to zero at the edge of contact, the ratio q/p becomes infinite there. Bental and Johnson, however, show that for rolling contact between a strip and a cylinder this ratio falls to zero at the edges of contact. Because of the discrete nature of our numerical analysis we are only able to examine this ratio at the $2S - 1$ points n . If full stick is assumed, the highest value of q/p predicted by our numerical solution with S set to 10 is 0.328 at $b/a = 0.343, |x|/a = 0.9$. Thus if $f < 0.328$, the solution produced by assuming adhesion everywhere is violated. If $f > 0.328$ possible violations may occur at $x/a > 0.9$ but cannot be detected without increasing S .

For values of f where violations occur an iterative scheme is adopted to overcome the problem. At each load increment stick is first assumed. The outer points are then checked for violations of the friction law and where these are detected Q_n is replaced by $\pm f P_n$ as appropriate. The matching of the tangential displacement is discarded within the new slip zone $c \leq |x| \leq a$ (Fig. 1(c)). A new solution is now obtained, and again checks for violations are carried out. If necessary, further points are permitted to slip until a satisfactory result is obtained. Values of $u(\pm c)$ are recorded for incorporation at the next load step, which can now be taken. Figure 6 shows the results obtained for $f = 0.2, \nu = 0.3$ with $S = 20$.

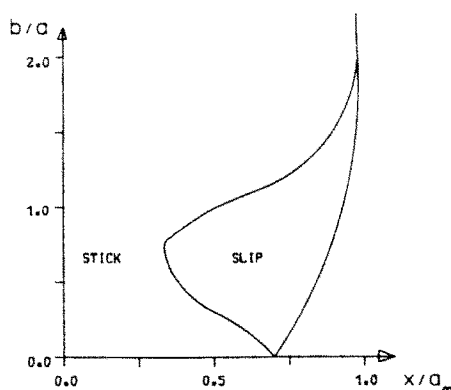


Fig. 7. Frictional indentation, $\nu = 0.3$, $f = 0.2$, stick and slip zones.

The variation of the stick zone boundaries and the size of the contact patch is shown in Fig. 7. It is seen that for $b/a \geq 2.0$ the contact is effectively Hertzian. As the load is increased the slip zones develop, reaching a maximum proportion of the contact at about $b/a = 0.6$. As the load is increased further the slip zone rapidly recedes so that as $b/a \rightarrow 0$ normal Hertzian conditions again apply.

MINDLIN PROBLEM

As stated at the outset, the object of the present work was to assess the influence of finite strip thickness on fretting fatigue analysis. The classical analysis of this configuration, with each body approximated by a half-plane was carried out by Mindlin[9]. In his solution two elastically similar bodies are pressed normally together so that they stick everywhere, and then a tangential force less than that needed to cause sliding is applied, giving rise to a central stick zone bordered by slip of the same sign.

In our configuration, slip zones of *opposite* sign already exist before the tangential force is applied. As soon as such a force is applied the magnitude of the shear stress on one side is augmented, whilst the other is reduced (Fig. 1(d)). This is accompanied by a small relative displacement in the direction of the augmented shear. Note, however, that in the slip zone where the shear traction is depleted, the shear traction and relative "slip velocity" are of opposite sign. This violates the friction law and hence instantaneous adhesion results ($-a < x < -c$, Fig. 1(d)). As the magnitude of Q is increased, we expect slip to re-start at $x = -a$, but to be of the same sign as that in the interval $c < x < a$.

The starting conditions for the solution of this loading are the final conditions for frictional indentation, but with an infinitesimal load increment δQ applied so that the stick zone extends over $-a < x < c$. The relative tangential displacement u is already known for $-c < x < c$ and may be calculated for $-a > x > -c$ using eqn (5). The application of a shear force Q results in a relative displacement δ_t between distant points in the bodies, so that the tangential matching condition expressing $\epsilon_r = \text{constant}$ becomes

$$u_m = u_{m0} + \delta_t \quad (9)$$

where u_{m0} are the values determined before Q is applied. The further unknown δ_t gives a measure of the tangential compliance. The problem is rendered determinate by introducing the second (tangential) equilibrium equation

$$\sum_{n=-(s-1)}^{s-1} Q_n = Q/\bar{p} = 2SQ/P. \quad (10)$$

Again an iterative solution is pursued. The required value of Q/P is chosen and the stick zone taken initially to be $-a < x < c$. If violations occur either or both outer points are allowed to slip and the problem re-solved. The method proceeds until a satisfactory solution is obtained. It should be noted that an incremental approach is not required since

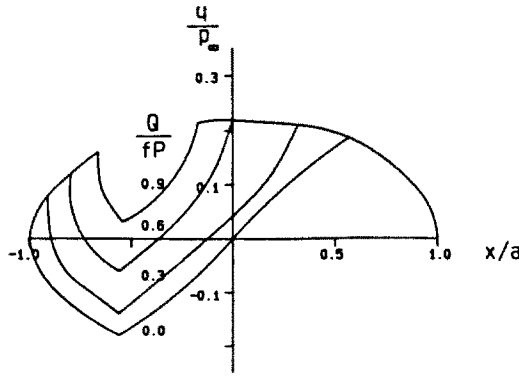


Fig. 8. Mindlin type contact, $\nu = 0.3$, $f = 0.2$, shear traction distributions.

the stick zone recedes and u_{m0} is known everywhere. Shear traction distributions for a range of values of Q/fP are given in Fig. 8 for $b/a = 1.0$, $f = 0.2$, and $\nu = 0.3$. For these values of b/a and f coupling between shear and direct tractions is so small that the direct tractions are almost identical to the case when $Q = 0$. Similarly the variation of a/a_0 with Q is sufficiently small to be neglected. Figure 9 summarizes the variation of stick zone boundaries with Q/fP for $b/a = 1.0$, $f = 0.2$, and $\nu = 0.3$.

CONCLUSION

A range of frictionless and frictional contact problems of an elastic strip indented by two rollers has been studied. For each, the interfacial tractions have been deduced using the method of Bentall and Johnson. It has been shown that the largest discrepancies from Hertzian theory occur at $b/a \approx 0.4$ and that if $b/a > 5.0$, differences are negligible. The results confirm that the contact pressure is still approximately parabolic (Figs 3, 5(a), and 6(a)) but that the contact size and peak pressure are considerably altered. Figure 10 may be used to calculate both these quantities for any known load since the equivalent Hertzian contact size a_0 is easily found. These results are presented for the case of adhesive indentation, but are almost identical for the other configurations studied.

The effect of finite strip thickness on the form of the contact pressure distribution for a sliding contact is slight (Fig. 4) and is very much less than the influence of a dissimilarity between elastic constants[10]. Indeed, a general result of all our investigations is that the effect of coupling between the shear and direct tractions is small. Said differently, it may be stated that for practically realizable coefficients of friction, the magnitude of surface vertical displacements induced by shear is much less than the initial curvature. Therefore it would be entirely reasonable, for all strip thicknesses, to solve directly for the pressure, neglecting the effect of $q(x)$. This would considerably facilitate the solution.

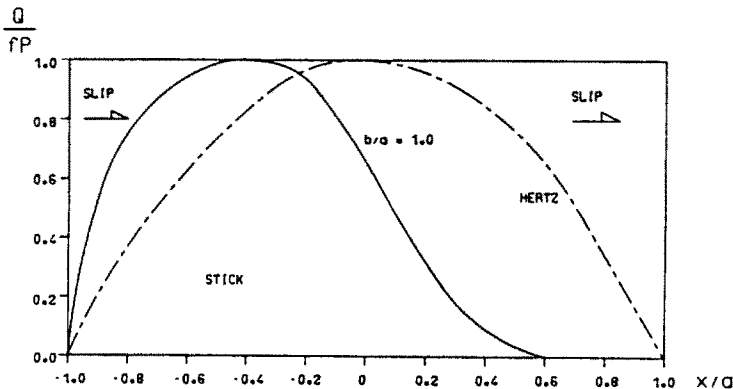


Fig. 9. Mindlin type contact, $\nu = 0.3$, $f = 0.2$, stick and slip zones.

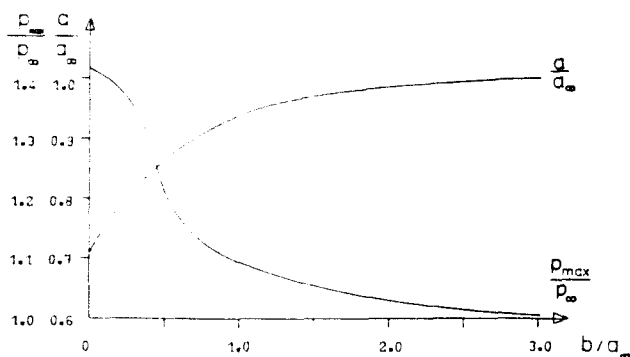


Fig. 10. Variation of contact size and peak pressure with normalized strip width, adhesive indentation, $\nu = 0.3$.

Adhesive and frictional indentation problems require an incremental solution, which is rather expensive in computing time but gives satisfactory results with $S = 10$ or greater. The effect of finite friction on the results is not significant at realistic values of f , as noted by Bentall and Johnson[4]. The effect on the direct traction is very small, being confined to a slight attenuation near the edges of contact and a corresponding increase at $x/a \approx 0.5$. There is, however, a more pronounced shift in the shear traction distribution towards the centre of contact (cf. Figs 5(a) and 6(a)).

Lastly, the effect of finite strip thickness on stick/slip zones for Mindlin contact has been found (Figs 8 and 9). It may be seen from Fig. 9 that one stick zone grows considerably at the expense of the other, affecting the amplitude of microslip, which is of considerable interest in the analysis of fretting fatigue. Stress fields have not been calculated here, but might be most conveniently done by utilizing expressions for the stresses induced by a triangular distribution of traction[3] and using superposition. Previous calculations of the stresses induced by a Mindlin contact modified by the presence of a bulk tension[2] indicate that the shifted stick zone is unlikely to have a large effect on the stresses in the strip, even at those strip thicknesses where there is substantial asymmetry. A similar problem of a finite strip indented by a rigid indenter has been studied by Keer and Farris[11].

Acknowledgement—David Nowell acknowledges the support of the SERC under contract No. GR/D55610.

REFERENCES

1. J. J. O'Connor, The role of elastic stress analysis in the interpretation of fretting fatigue failures. In *Fretting Fatigue* (Edited by R. B. Waterhouse), Chap. 2. Applied Science, Barking (1981).
2. D. Nowell and D. A. Hills, Mechanics of fretting fatigue tests. *Int. J. Mech. Sci.* **29**, 355-365 (1987).
3. I. N. Sneddon, *Fourier Transforms*. McGraw-Hill, New York (1951).
4. R. H. Bentall and K. L. Johnson, An elastic strip in plane rolling contact. *Int. J. Mech. Sci.* **10**, 637-663 (1968).
5. N. I. Muskhelishvili, *Some Basic Problems of the Mathematical Theory of Elasticity* (Translated by J. R. M. Radok). Nordhoff, Groningen (1953).
6. D. A. Spence, Self-similar solutions to adhesive contact problems with incremental loading. *Proc. R. Soc. A*, **305**, 55-80 (1968).
7. D. A. Spence, The Hertz contact problem with finite friction. *J. Elasticity* **5**(3-4), 297-319 (1975).
8. L. E. Goodman, Contact stress analysis of normally loaded rough spheres. *J. Appl. Mech.* **29**(3), 515-522 (1962).
9. R. D. Mindlin, Compliance of elastic bodies in contact. *J. Appl. Mech.* **16**, 259-268 (1949).
10. D. A. Hills and A. Sackfield, Sliding contact between dissimilar elastic cylinders. *J. Tribology* **107**, 463-466 (1985).
11. L. M. Keer and T. N. Farris, Effects of finite thickness and tangential loading on development of zones of microslip in fretting. *Trans. ASLE* (1988), in press.

APPENDIX: INFLUENCE FUNCTIONS

$$I_{wi} = \frac{2}{z} \int_0^z \left[\frac{1 - \cosh \beta}{\beta + \sinh \beta} \right] \sin^2 z\beta \frac{d\beta}{\beta^i}$$

$$I_4[n] = \frac{-4}{z} \int_0^{\pi} \left[1 + \frac{1 - \cosh \beta}{\beta + \sinh \beta} \right] \sin^2 z\beta \sin^2 n z\beta \frac{d\beta}{\beta^3}$$

$$I_5[n] = \frac{-2}{z} \int_0^{\pi} \left[\frac{\beta}{\beta + \sinh \beta} \right] \sin^2 z\beta \sin 2nz\beta \frac{d\beta}{\beta^3}$$

$$I_{4a}[n] = \int_0^{\pi} \sin^2 \beta \sin^2 n\beta \frac{d\beta}{\beta^3}$$

$$I_{5a}[n] = \int_0^{\pi} \sin^2 \beta \sin 2n\beta \frac{d\beta}{\beta^3}$$

$$I_6[n] = \frac{-4}{z} \int_0^{\pi} \left[1 - \frac{1 + \cosh \beta}{\beta + \sinh \beta} \right] \sin^2 z\beta \sin^2 n z\beta \frac{d\beta}{\beta^3}$$

$$z = \frac{a}{4st}$$